

THE 4X SOURCE*

H. Vernon Smith, Jr., Paul Allison, and Joseph D. Sherman, AT-2, MS H818
Los Alamos National Laboratory, Los Alamos, NM 87545 USA

Summary

Our Penning surface-plasma source (SPS) discharge chamber was enlarged 4X in two dimensions. To date, three pulsed discharge modes have been studied: two with noisy arc ($\geq 20\%$ H^- current fluctuations) and one with quiescent arc ($< 1\%$ H^- current fluctuations). Lower arc magnetic field and higher H_2 gas flow allow switching from the noisy to the quiescent mode. The noisy modes yield up to 120 mA of 29-keV H^- beam; for 110 mA at 29 keV, the two-dimensional normalized rms emittance is $0.017 \times 0.018 \pi \cdot \text{cm} \cdot \text{mrad}$. The quiescent mode yields 75 mA of 29-keV H^- beam; for 67 mA at 24 keV, the emittance is $0.011 \times 0.012 \pi \cdot \text{cm} \cdot \text{mrad}$.

Introduction

We initiated work on the 4X source when we realized that transporting the H^- beam from the source to a radio-frequency quadrupole (RFQ) accelerator probably would be better accomplished with a circularly symmetric beam rather than the slit beam from the source¹ now used, called the small-angle source (SAS) because of its small bending angle for the extracted H^- beam. It was necessary to increase the size of the SAS discharge chamber to accommodate the 5.4-mm-diam circular emitter that the beam-optics criteria indicated we needed to produce a $0.01 \pi \cdot \text{cm} \cdot \text{mrad}$ emittance for our assumed H^- ion temperature of 4 eV. In addition, to make an intense dc H^- ion beam with the Penning SPS, we must lower the electrode power loading from the 7-16 kW/cm^2 observed in the SAS¹ to values closer to 1 kW/cm^2 . We are working toward both goals with a source scaled up 4X in size over the SAS, hence the name 4X source.

SNOW² predicts that the emitter-extractor configuration shown in Fig. 1 of Ref. 3 will produce a 160-mA H^- beam at 29 keV having an rms emittance of $0.0089 \pi \cdot \text{cm} \cdot \text{mrad}$ and an rms divergence angle of 55 mrad for an ion temperature $kT = 4$ eV. Fluctuations in H^- current produce changes in the ion trajectories. Using the concept of mismatch factor,⁴ the time-averaged emittance growth is 70% for $\pm 10\%$ current fluctuations. We design for $0.015 \pi \cdot \text{cm} \cdot \text{mrad}$ because we observe fluctuations of $\leq 10\%$ on the H^- beam current from the SAS, and we want to keep the beam emittance below our previously achieved $0.02 \pi \cdot \text{cm} \cdot \text{mrad}$, if possible. A schematic of the 4X source is shown in Fig. 1. The bend angle, 4.6° , is as small as practical to allow close coupling to an accelerating column to minimize beam-transport emittance growth. The 4X source design is described in Ref. 3, and a preliminary report of 4X source results is given in Ref. 5. After the work in Ref. 5 was completed, the extraction-electrode aperture was increased from 3.6- to 4.4-mm diam. An independently controlled oven containing about 0.5 cm^3 of a compressed titanium-cesium chromate mixture (two parts Ti to one part Cs_2CrO_4 by weight) is heated to 350-400°C to supply cesium vapor to the arc.

Results

We varied the arc magnetic field \bar{B}_x and measured the emittances ϵ_x and ϵ_y . There should be no magnetic-field dispersion of the H^- ions in x because the magnetic field is in the x-direction. These data were taken with the x- and y-emittance scanners⁶ 10.6 and 33.9 cm, respectively, from the source emission

*Work supported by the US Air Force Office of Scientific Research.

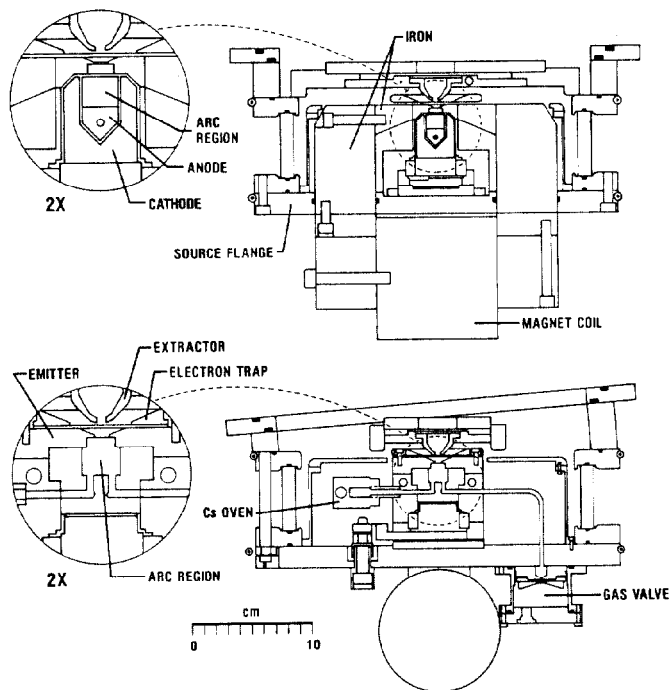


Fig. 1. Schematic of the 4X source. Top view: arc magnetic field in the plane of the paper; lower view: arc magnetic field direction (x) out of the paper. At the left are 2X enlargements of the arc region.

aperture. A Xe density of about $3 \times 10^{12} \text{ cm}^{-3}$ was present in the vacuum chamber to prevent emittance growth of the beam in transport to the y-emittance scanner. Our previous experience¹ with transport of a high-perveance H^- beam shows that emittance will increase in transport unless a relatively high-density background gas is used to help neutralize the beam; Xe is the best neutralizing gas. The 4X source discharge was run in the 300-V, 85-A mode (Mode I, Table I) for these measurements. There is no evidence for any variation of ϵ_x or ϵ_y with B_x (Fig. 2), considering that the emittance measurements have uncertainties on the order of 10%. There is only a small difference (2%) between ϵ_x measured with and without Xe in the vacuum box; therefore, we do not think the presence of the Xe affects the trend of the ϵ_y -measurements or the conclusion that there is no observable effect of source magnetic field on the ϵ_y -values.

For Arc Mode I (Table I) and 29-kV extraction voltage, we obtained 110 mA of H^- at the Faraday cup 5.6 cm from the emitter (Fig. 8 of Ref. 5 shows a schematic of the 4X source, Faraday cup, and emittance scanners). The e^-/H^- extracted-current ratio was 1.5/1. The phase-space density contours for the y-plane are shown in Fig. 3. The emittance of this beam is $0.017 \times 0.018 \pi \cdot \text{cm} \cdot \text{mrad}$. The beam noise level is about $\pm 25\%$ (measured on an oscilloscope with a 50-MHz bandwidth).

A second noisy mode (Mode II, Table I) has a discharge voltage of 130 V. Preliminary measurements give $\epsilon_x \times \epsilon_y$ values of $0.022 \times 0.023 \pi \cdot \text{cm} \cdot \text{mrad}$ for a 100-mA, 29-keV H^- beam from Mode II. The beam noise level is about $\pm 20\%$; the e^-/H^- ratio, about 3.3/1.

We can attain a quiescent arc (Mode III, Table I) and H^- beam (Fig. 4) by increasing the pulsed H_2 gas flow and then decreasing the arc magnetic field. Arc

TABLE I
4X SOURCE PULSED-ARC MODES

	Mode I	Mode II	Mode III
Discharge voltage, V	300	130	540
Discharge current, A	85	180	50
Magnetic field, T	0.15	0.15	0.07
Pulsed gas ₃ flow, std. cm ³ /min	170	230	260
Discharge voltage noise (peak-to-peak)	±10% incoherent	±40%, 4 MHz coherent oscillations	<±1%
H ⁻ current, mA	110	100	67
H ⁻ beam energy, keV	29	29	24
H ⁻ beam noise (peak-to-peak)	±25%	±20%	≤±1%
ϵ_x , $\pi \cdot \text{cm} \cdot \text{mrad}$	0.017	0.022	0.011
ϵ_y , $\pi \cdot \text{cm} \cdot \text{mrad}$	0.018	0.023	0.012
H-atom energy, eV ^a	2.0	2.6	2.3

^aFrom Ref. 7.

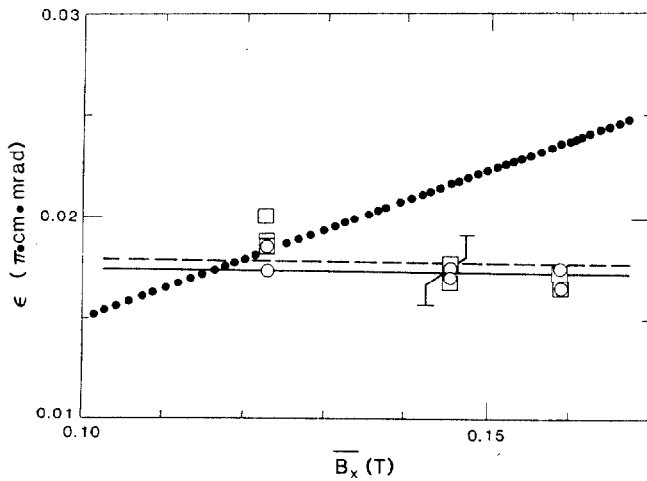


Fig. 2. Measured rms emittance ϵ versus arc magnetic field B_x for Mode I. The squares and dashed line are for the y-plane, the circles and solid line are for the x-plane. The dashed and solid lines are a guide to the eye and represent the averages of the measurements for the two planes. The dotted line is ϵ_y versus B_x calculated by combining Eqs. (1) and (2) and using $D = 12$ mm. A representative error bar is shown on the graph. Note the suppressed zero on the horizontal and vertical scales.

Mode III produced 67 mA of H⁻ beam at 24 keV. The y-plane phase-space density contours are shown in Fig. 5. The y-emittance scanner was 10.6 cm from the emission aperture for the Mode II and III measurements with no Xe gas added to the vacuum box. The H⁻ beam emittance is $0.011 \times 0.012 \pi \cdot \text{cm} \cdot \text{mrad}$. The H⁻ beam current increases to only 75 mA when the extraction voltage is raised to 29 keV, indicating that at this arc current, the H⁻ current is limited by H⁻ production in the source plasma rather than by space-charge effects in the extraction gap. The e⁻/H⁻ ratio is 1.5/1. The beam-fluctuation amplitude is $\leq \pm 1\%$.

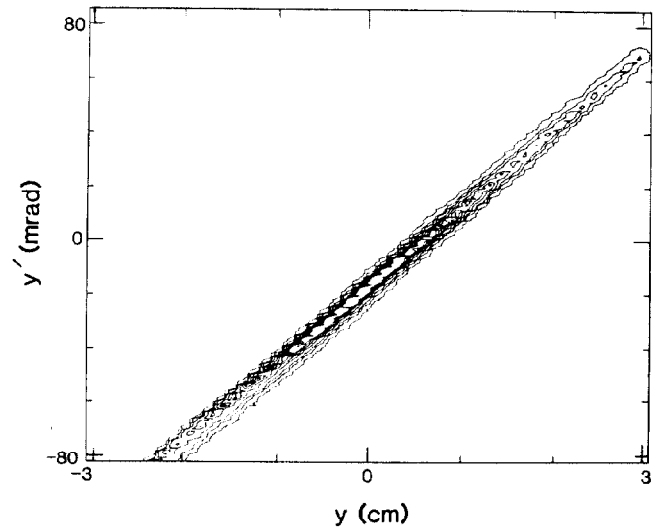


Fig. 3. The y-plane phase-space density contours for Mode I at the 1, 5, 10, 20, 30, 40, and 50% levels.

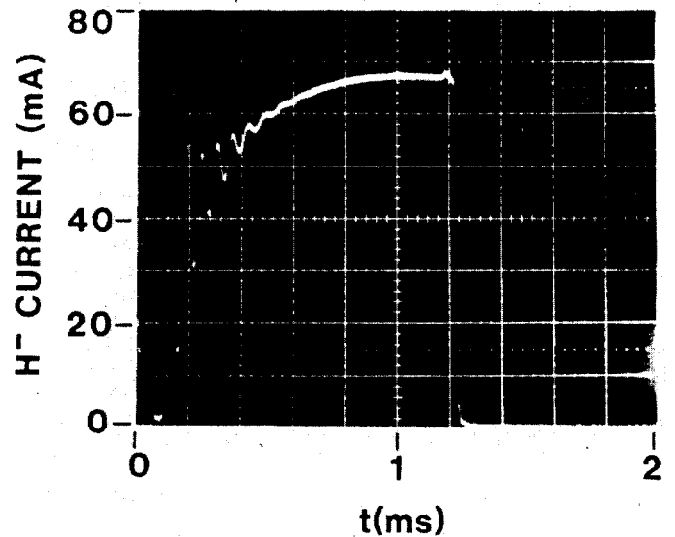


Fig. 4. Quiescent Mode III H⁻ current waveform. The H⁻ energy is 22 keV and oscilloscope bandwidth is 50 MHz for this oscillogram.

Discussion

There are at least five possible sources of emittance for our extracted H⁻ beam: actual H⁻ ion temperature in the plasma, aberrations in the extraction system, nonlinear space-charge compensation effects in the beam transport, magnetic dispersion of the H⁻ ions, and increase in the time-averaged emittance caused by perveance (current) fluctuations in the extraction gap. The H-atom temperature in the source plasma has been determined⁷ for each of the three pulsed discharge modes using optical spectroscopy (Table I). The resulting emittance ϵ , calculated from a model⁸ that assumes a Maxwellian energy spread characterized by temperature kT for the beam extracted from a circular emitter of radius R , is

$$\epsilon_{x,y} = (R/2)(kT/mc^2)^{1/2} \quad (1)$$

where m is the ion mass. If we assume that the H⁻ ions have the same temperature (2 eV) as the H atoms, then $\epsilon_{x,y} = 0.006 \pi \cdot \text{cm} \cdot \text{mrad}$ for $R = 0.27$ cm.

It is unlikely that extraction-system aberrations produce the balance of the measured emittance, 0.017-0.023 $\pi \cdot \text{cm} \cdot \text{mrad}$, for noisy Modes I and II because our SNOW calculations predict 0.007 $\pi \cdot \text{cm} \cdot \text{mrad}$.

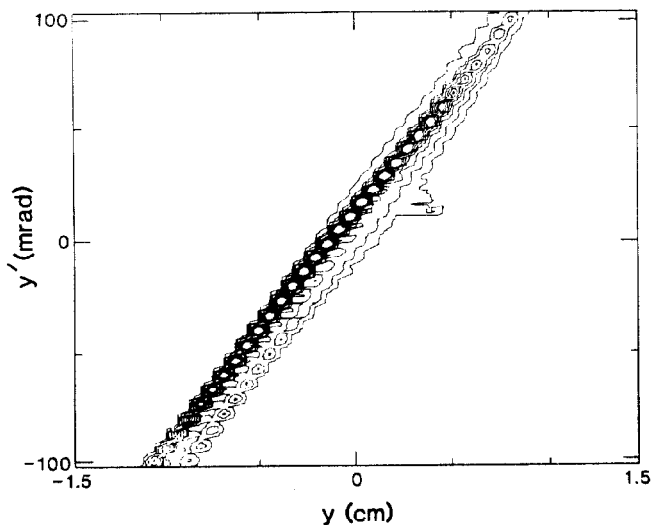


Fig. 5. The y -plane phase-space density contours for Mode III at the 1, 5, 10, 20, 30, 40, and 50% levels.

Extraction-system aberrations may account for the rest of the measured emittance, $0.011 \pi \cdot \text{cm} \cdot \text{mrad}$, for quiescent Mode III. Space-charge effects in beam transport are unlikely to contribute significantly because we note only about 2% change in the emittance measured 11 cm from the source with and without Xe neutralizing gas.

The effective dispersion-plane (y) H^- ion temperature kT_y may be increased by the variation in transverse momentum imparted by the average-source magnetic field B_x as the ions of mass m cross the production region of width D .

$$kT_y = (e \bar{B}_x D)^2 / 12m \quad (2)$$

The mechanical width for the 4X source is 12 mm if the 4-mm drift from the plasma to the emission aperture is ignored. The effective width may be lower than the mechanical width because of charge exchange or stripping losses of H^- ions in the source plasma. The kT_y value calculated from Eq. (2) ($B_x = 0.161$, $D = 12$ mm) is 29 eV, somewhat higher than the 16-eV effective ion temperature calculated from Eq. (1) ($\epsilon_{x,y} = 0.018 \pi \cdot \text{cm} \cdot \text{mrad}$, Fig. 2). There appears to be no variation of $\epsilon_{x,y}$ or kT with magnetic field (Fig. 2), indicating that the origin of emittance is not magnetic dispersion. We cannot exclude magnetic-dispersion effects as the origin of emittance for Modes II and III because we have not examined the variation of emittance with magnetic field for these modes.

The remaining effect is perveance fluctuations in the extraction gap caused by the current fluctuations on the H^- beam. Using the mismatch factor⁴ and SNOW results to calculate the emittance growth for the noisy and quiescent beams having $\pm 20\%$ and $\pm 1\%$ current fluctuations, respectively, predictions for emittance growth of 140% and 4% result. Thus, this effect can explain the added noisy beam emittance, but cannot be the origin of the quiescent beam emittance. More detailed work is needed to determine the origins of both the noisy and quiescent beam emittances. We consider it likely that the quiescent mode emittance is determined by only the H^- source plasma temperature and extraction system aberrations, in roughly equal measures. The noisy-mode emittances probably are dominated by perveance fluctuations in the extraction gap.

Possibly the quiescent mode is obtained by adjusting the arc parameters so that the loss of electrons to the anode by classical diffusion equals the loss of ions to the cathode, without nonclassical transport

mechanisms (oscillations) being necessary to achieve the particle balance. From Eq. (9) in Ref. 9, we derive the condition

$$BW/2 = 9.2 \sqrt{\sigma L n_n kT_e m_e / e^2} M^{1/4} \quad (3)$$

which the product of the arc magnetic field B and arc slot width W must satisfy for quiescence. In Eq. (3), σ is the electron neutral cross section ($\sim 10^{-15} \text{cm}^2$), L is the cathode-cathode gap, n_n is the neutral-particle density (assumed to be $4 \times 10^{15} / \text{cm}^3$), and $M = 1, 2,$ or 3 for $\text{H}^+, \text{H}_2^+,$ or H_3^+ , respectively. For the SAS, the observed $BW/2$ is about 0.15 T-mm for H^+ . Using $kT_e = 2$ eV in Eq. (3) gives 0.04 T-mm. For the 4X source with $kT_e = 2$ eV, Eq. (3) also gives 0.04 T-mm, but our observed $BW/2$ is 0.1 T-mm for dc and 0.3 T-mm for pulsed operation.

The electrons that accompany the extracted H^- beam will pose a problem for a dc source. We have an e^-/H^- ratio of as low as 1.5/1 for the extracted particles. A method of suppressing the electrons, or collecting them at low energies, may be needed before a successful dc source, based on the 4X source, can be operated. An electron trap was designed with the 4X source (Fig. 1), but it has not been tried.

The electrode power loading is important because it will determine the 4X source scale-up required to produce a 160-mA dc H^- beam. Basing our estimate primarily on Mode I for the 110-mA, 29-keV H^- beam ($P_{\text{cathode}} = 3-6 \text{ kW/cm}^2$), another scale-up of about 4X (for a total scale-up of 16X over the SAS) is necessary to reach 1 kW/cm^2 .

We measure perveance versus extraction voltage for Modes II and III. The maximum perveance is 72% of the value calculated using SNOW. It is unlikely that electron loading in the gap is responsible for the 28% reduction from the limit because we calculate that an electron loading five times the H^- loading causes only a 10% decrease in perveance. The likely cause of the perveance reduction is gas stripping of the H^- beam in the beam transport.

Future Work

Future work on the 4X source will focus on attaining quiescent operation with lower arc voltage. Still to be done are detailed studies of the measured H^- beam optical properties compared with the SNOW-code predictions. Also, a scheme to handle the electron loading of the extractor in a dc-source design needs to be devised. The arc pulser has been modified to deliver more arc current in an attempt to increase the H^- current from the high-voltage quiescent arc mode.

References

1. P. Allison and J. D. Sherman, "Operating Experience With A 100-keV, 100-mA H^- Injector," AIP Conf. Proc. No. 111, AIP, New York (1984), 511-518.
2. J. E. Boers, "SNOW - A Digital Computer Program for the Simulation of Ion Beam Devices," Sandia National Laboratory report SAND79-1027, 1980.
3. H. V. Smith, Jr., P. Allison, and J. D. Sherman, "A Scaled, Circular-Emitter Penning SPS for Intense H^- Beams," AIP Conf. Proc. No. 111, AIP, New York (1984), 458-462.
4. Paul Allison, "Emittance Growth Caused by Current Variation in a Beam-Transport Channel," these proceedings.
5. H. V. Smith, Jr., P. Allison, and J. D. Sherman, "The 4X Source," Los Alamos National Laboratory document LA-UR-84-1843, June 1984.
6. P. W. Allison, J. D. Sherman, and D. B. Holtkamp, "An Emittance Scanner for Intense Low-Energy Ion Beams," IEEE Trans. Nucl. Sci. **30** (4) (1983), 2204-2206.
7. R. Keller and H. V. Smith, Jr., "Spectroscopic Measurements on an H^- Ion Source Discharge," these proceedings.
8. J. D. Lawson, "The Physics of Charge-Particle Beams," (Clarendon Press, Oxford, 1977), 201. P. Allison, J. D. Sherman, and H. V. Smith, Jr., "Comparison of Measured Emittance of an H^- Ion Beam With a Simple Theory," Los Alamos National Laboratory report LA-8808-MS (June 1981).
9. L. Jerde, S. Friedman, W. Carr, and M. Seidl, "Plasma Quiescence in a Reflex Discharge," J. Appl. Phys. **51** (1980), 965-969.